AADE-26-FTCE-073

Mechanical Integrity of Alternative Cementing Materials for CCS Environments

Athar Hussain, ProPetro Services; Grant Kuwata, Diana Maury Fernandez, Sugan Raj Thiyagarajan, Hossein Emadi, Texas Tech University; Conrad Longman and Ahmed Mansour, ProPetro Services

Abstract

This study examines the mechanical behavior of alternative well cementing materials following exposure to supercritical CO_2, crucial for maintaining wellbore integrity in carbon capture and storage (CCS) projects. The primary focus is on assessing the impact of CO_2 exposure on the porosity, and mechanical properties of these materials, which serve as key barriers against leakage. This research aims to evaluate alternative cementing solutions' long-term performance and suitability in subsurface storage environments.

Three distinct cementing formulations were tested: a neat class H cement, a resin cement blend, and a Class F Fly Ash Geopolymer. Cylindrical samples (3 in x 1.5 in) of each material were initially cured at 120°F for 7 days. Subsequently, the samples were exposed to supercritical CO_2 at 1500 psi and 120°F for 56 days. Before and after this treatment, the samples' porosity and triaxial compression tests at confining pressure of 1500 psi were conducted, to determine changes in strength and static elastic properties.

The results revealed that the porosity of all cement samples experienced minimal changes following the exposure. Notably, the Geopolymers exhibited a different behavior pattern compared to the conventional cement and resin cement, suggesting a unique interaction with supercritical CO_2. Despite the changes in porosity and material-specific responses, changes in peak strength were less than 10% for the samples. The findings suggest that the tested alternative cementing materials maintain their structural integrity under supercritical CO_2 exposure, indicating their potential for ensuring long-term wellbore stability in CCS applications.

Introduction

Carbon capture and storage (CCS) projects are critical for cutting CO_2 emissions by capturing CO_2 at source and placing it in secure underground reservoirs, often depleted oil and gas fields that offer suitable geology for long-term containment. Ensuring these reservoirs remain secure requires careful assessment of leakage risks, particularly from legacy wells that were drilled and abandoned before modern CO_2-focused standards existed. Evidence indicates purpose-built CO_2 and acid-gas injection wells fail less often than repurposed or improperly abandoned wells, so strict drilling, completion, and abandonment protocols aligned with robust regulations are essential to reduce leakage probability. The casing–cement–formation assembly must remain intact because multiple escape routes for CO_2 can develop around the wellbore (Figure 1). Common failure modes include debonding at the rock–cement and cement–casing interfaces and internal cement cracking, each of which can create a connected pathway for fluid migration. CO_2 is usually injected in a supercritical phase, which enables it to mix readily with formation brines and form carbonic acid. CO_2-rich brine with a pH below about 4 can move into cement pore networks and react with the cement's alkaline pore fluid, triggering dissolution and secondary mineral transformations. These reactions accelerate cement deterioration: calcium is leached from the hydrate phases and can be replaced by amorphous silica-rich residues that weaken the microstructure and change porosity and permeability. Such chemical alteration of the annular cement raises significant questions about the durability of well seals and the long-term security of CO_2 storage.

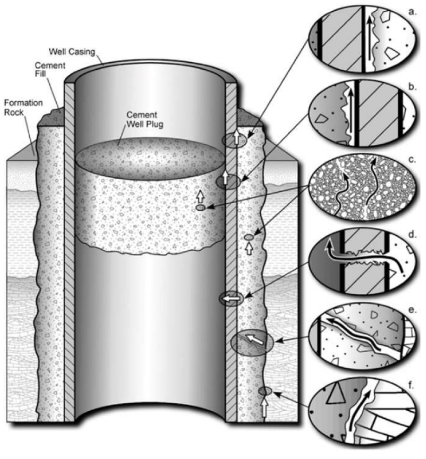

Figure 1 Common Wellbore Leakage Pathways (Gasda et al.,2004)

Studies on Class G and H well cements demonstrate that carbonation penetration is highly sensitive to curing regime, test setup, and solution chemistry, producing a wide span of alteration depths under different conditions. For example, Class G cores exposed at 90 °C and 30 MPa developed a carbonation front that advanced roughly 1.1 mm in 84 hours, with metastable calcium carbonate phases forming at the reaction interface (Corvisier et al., 2010). Longer-term, forced-transport experiments show varied damage profiles—after five weeks, alteration depths of about 800 µm at the cathode and 200 µm at the anode were recorded—illustrating how transport-driven processes produce asymmetrical degradation. Accelerated tests under supercritical CO_2 further underline the potential for substantial long-term penetration: Class H cement specimens cured for 28 days exhibited progressive carbonation that models predict could reach about 1.68 mm over a 30-year timescale (Strazisar et al., 2009). Formulations containing pozzolanic constituents respond even faster in aggressive CO_2 environments; a 35:65 pozzolan-to-cement mix has been shown to achieve approximately 5 mm carbonation depth and near-complete reaction within two days under intensified exposure, indicating that supplementary materials can both change reaction pathways and accelerate alteration. Temperature and brine composition also strongly influence microstructural and physical-property changes: comparative tests at ambient and elevated temperatures (e.g., 50 °C) with increased salinity report significant differences in penetration depth and resulting cement integrity (Carroll et al., 2016; Kutchko et al., 2008). Collectively, these findings emphasize the need to account for curing history, material composition, thermal state, and fluid chemistry when predicting carbonation behavior and designing cementitious barriers for CO_2 storage applications.

Resin-based wellbore barriers present an alternative approach: engineered resins, developed since the 1860s and adopted in oilfield use about 80 years later, offer strong adhesion, resistance to corrosive fluids, low unset viscosity for placement, and toughness and flexibility after curing. Properly formulated resins continuously transmit hydrostatic pressure to the formation during transition from liquid to solid, forming an impermeable seal when cured. Practical deployment requires formulations that can be easily mixed and pumped downhole without prematurely gelling, while avoiding exothermic reactions with formation water that could damage downhole environments or surface equipment. This study therefore assesses resin-based annular barrier concepts and compares their potential to withstand supercritical CO_2 exposure and maintain well integrity against conventional cement blends under aggressive reservoir conditions.

Methodology

Experimental Setup

Neat class H cement slurry was prepared according to API-RP-10B-2 specifications (API, 1997), using a water to cement ratio of 0.38. The slurry was poured into cylindrical steel molds after mixing and was cured for 72 hours at 120°F and atmospheric pressure. After the curing period, the cement samples were dried for 24 hours in a vacuum oven at 120°F. Then, porosity, elastic properties, Young's modulus and Poisson's ratio of the samples were measured.

The experimental arrangement for this work is illustrated in Figure 2. Cement specimens were mounted in a core-holder and exposed to supercritical CO_2 at 120 °F and 1500 psi for 56 days, with pressure continuously held and logged. Prior to exposure, the core-holder was evacuated with a vacuum pump to remove air, and after the CO_2 cycle specimens were stored in sealed containers to limit reaction with atmospheric moisture.

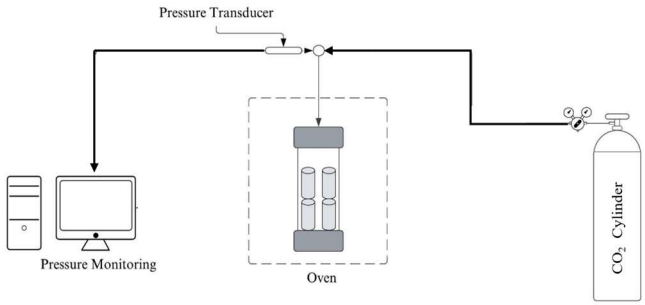

Figure 2 Experimental Setup

Porosity

Porosity was measured on each sample before and after CO_2 exposure using an Ultra-porosimeter 300 (Figure 3) and the Boyle's Law double-cell method for grain volume.

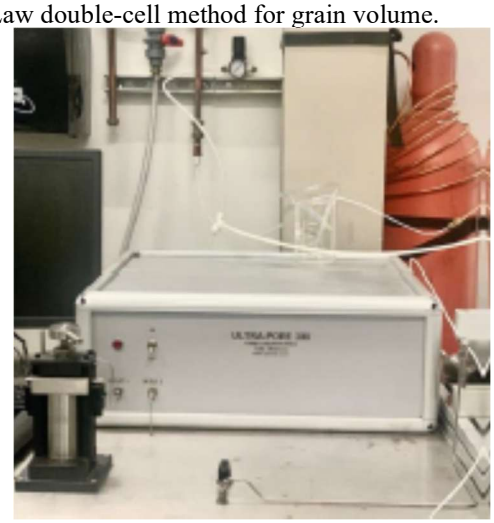

Figure 3 Ultra-Porosimeter 300

Triaxial Testing

Mechanical testing employed a triaxial system fitted with one circumferential and two axial strain gauges to simplify data collection and test control; specimens were prepared with self-fusing silicone electrical tape and a heat-shrinkable FEP membrane to prevent direct contact between the confining fluid and the sample and to avoid artefacts that could alter mechanical response (Figure 4).

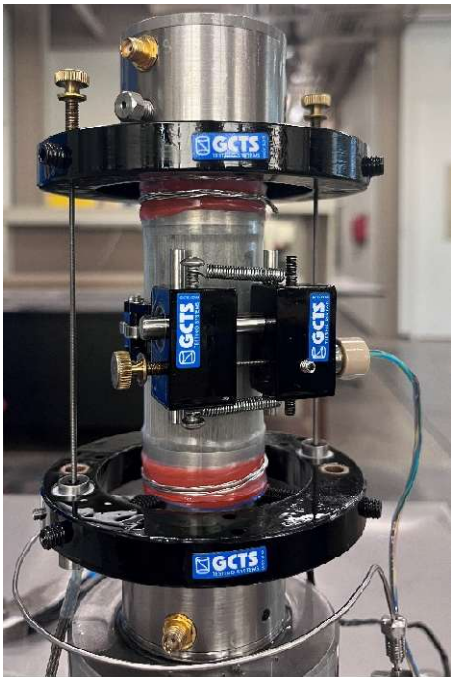

Figure 4 Cement sample prior to triaxial testing

During triaxial loading the cell maintained a confining pressure of 1500 psi while axial loading proceeded at a strain rate of 5×10^{-7} in/in/s. Each specimen was instrumented with two axial and one circumferential extensometers to record axial strain (εa), radial strain (εr) and volumetric strain (εv). From the stress–strain data the test provides axial deviatoric stress (Sd), peak strength, the static Young's modulus (E) from the tangent slope, and a dynamic estimate of Poisson's ratio (ν) derived from εa and εr. The GCTS RTR-2500 Rapid Rock Triaxial Testing System used for these experiments is shown in Figure 5.

Figure 5 Triaxial Testing System

Results

Porosity

Porosity measurements (Figure 6) indicate that the Class H cement consistently lost pore volume after exposure to supercritical CO_2, showing roughly a 14% reduction, while the geopolymer (fly ash–based) cement's porosity rose from 24.7% to 32.6%. In Portland-type cements, CO_2 reacts with calcium hydroxide in the matrix to form calcium carbonate, which can precipitate inside pores and thereby reduce overall porosity (Panduro et al., 2020; Strazisar et al., 2009). By contrast, the geopolymer's fly ash content — rich in amorphous aluminosilicates and lime — follows different carbonation pathways: CO_2-driven reactions can dissolve certain phases and produce secondary, often more porous minerals (for example ettringite under some conditions) instead of uniformly filling voids with $CaCO_3$, resulting in new interconnected pore networks and a net increase in porosity (Ati, 2004; Syahrir Ridha et al., 2020). The resin cement samples exhibited no significant change after supercritical CO_2 exposure. In contrast to the porosity values of the Class H and Geopolymers, the resin cement has very low porosity. Resin cement exhibits zero porosity because its dense polymer network fills all voids during polymerization, resulting in no pores, which allows it to show elastic behavior by returning to its original shape after stress.

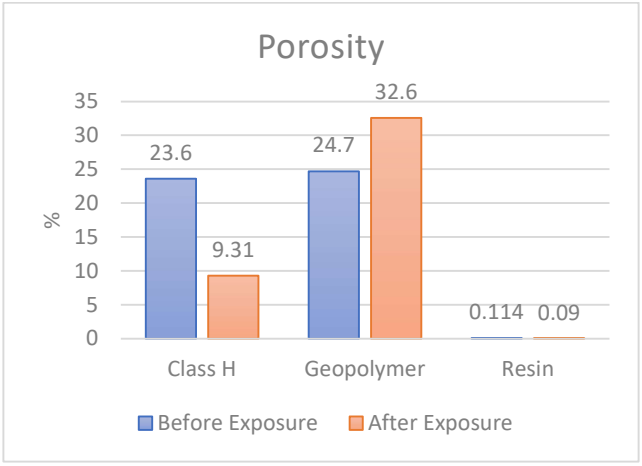

Figure 6 Porosity Results

Peak Strength, Young's Modulus and Poisson's Ratio

Porosity measurements and mechanical tests indicate that peak compressive strength (Figure 7), Young's modulus and Poisson's ratio (Table 1) change after CO_2 exposure in ways that correlate inversely with porosity. Class H samples, which lost porosity after treatment, display increases in peak strength and stiffness, whereas specimens with increased pore volume show reduced mechanical properties. Comparative studies report that supercritical CO_2 accelerates carbonation relative to natural exposure and produces a different pore-size distribution:

supercritically carbonated pastes contain a larger proportion of gel-scale pores (<10 nm) than air-carbonated counterparts. Because mechanical behaviour depends not just on total porosity but on pore geometry and connectivity, two samples with equal porosity can have different strengths if one has predominantly finer pores; cementitious materials with a 3D pore network typically become stronger when pore sizes decrease even if porosity is similar. Resin cement, being more elastic than Class H well cement, will generally show lower peak (ultimate) strength, a lower Young's modulus (i.e., it is less stiff and deforms more under the same stress), and a higher Poisson's ratio than Class H; Class H cement is formulated to be stiffer and stronger in compression (higher modulus and peak strength) and typically has a lower Poisson's ratio (around 0.2–0.3), whereas resin-based materials can tolerate larger elastic strains and exhibit more lateral strain for a given axial strain, producing a relatively higher Poisson's ratio.

Table 1 Poisson's Ratio and Youngs Modulus results.

Cement	Poisson's Ratio		Youngs Modulus (10^6 psi)	
	Pre Exposure	Post Exposure	Pre Exposure	Post Exposure
Geopolymer	0.26	0.16	1.48	1.32
Class H	0.21	0.22	1.63	3.22
Resin	0.55	0.52	0.26	0.31

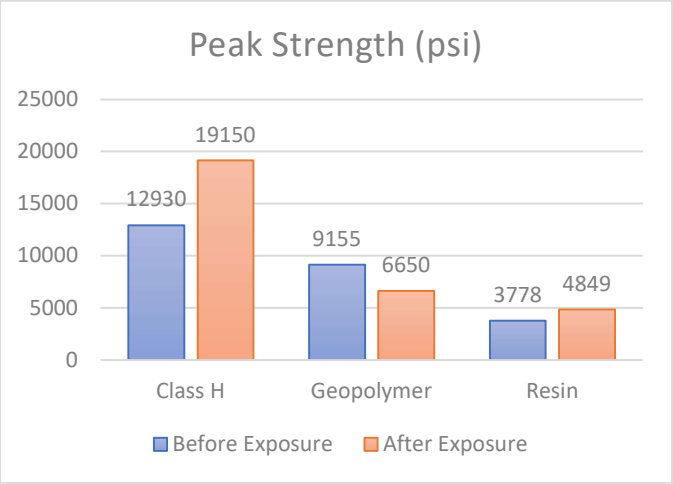

Figure 7 Peak Strength of the Tested Samples

The mechanisms underlying strength changes are microstructural. Precipitation of $CaCO_3$ microcrystals during carbonation can occlude interfibrillar spaces within outer C–S–H and at the interfacial transition zone, producing a denser solid matrix and enhancing load-transfer capacity. Under confining pressure, this densification reduces microcrack nucleation and growth, increasing peak strength; confining stress further restrains lateral dilation and limits damage propagation. Although some dissolution of phases may temporarily increase permeability, the remaining compact matrix and interconnected pore morphology can distribute stresses more evenly and reduce stress concentrations, so overall mechanical stability under confinement commonly improves (García-González et al., 2007; Sauki & Irawan, 2010).

Deviatoric Stress vs Strain Curves

Triaxial test results reflect the microstructural differences between the pre and post exposed samples. Deviatoric stress versus axial/radial strain curves show that unexposed reference samples usually have higher pre-yield stiffness and a more progressive post-peak softening, whereas CO_2-exposed specimens can exhibit altered yielding and either sharper or different post-peak declines depending on pore modification (Figure 8, Figure 9, Figure 10, Figure 11, Figure 12, Figure 13). The axial load responses of exposed geopolymer specimen increase markedly with microstrain — implying improved axial capacity — while radial stress–strain responses rise more slowly, revealing anisotropic effects of exposure on structural behaviour. Volumetric strain trends also shift: increased axial compression relative to lateral expansion produces net compaction (rightward shift on volumetric-strain plots), indicating reduced dilatancy and a transition from elastic to plastic, shear-accommodating deformation. This rearrangement of the cement matrix allows larger strains to be absorbed without immediate crack propagation, explaining improved post-exposure performance in some samples.

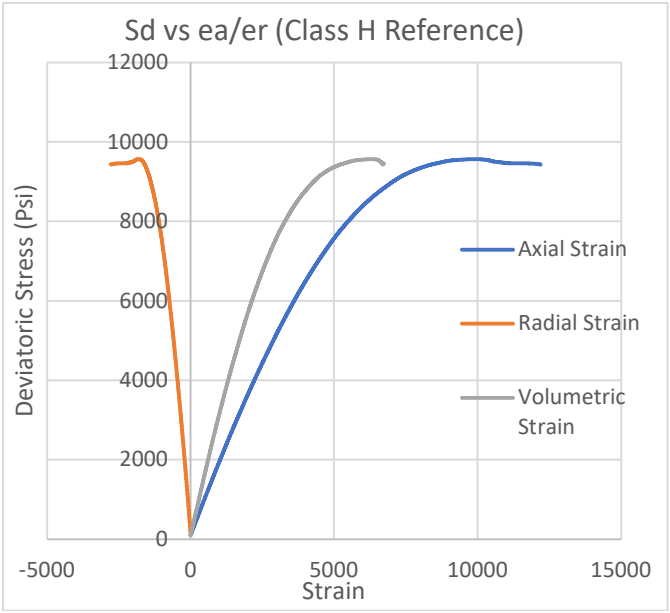

Figure 8 Stress vs Strain curve - Class H Reference

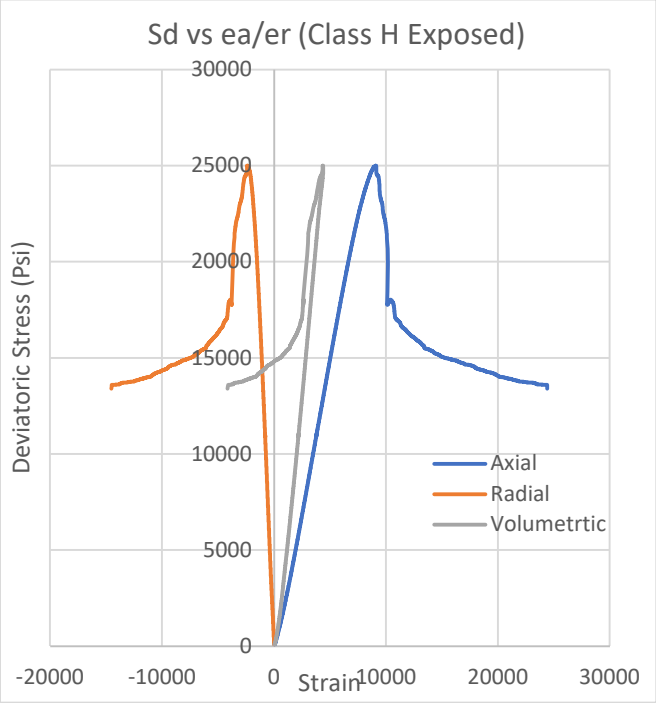

Figure 9 Stress vs Strain curve - Class H Exposed

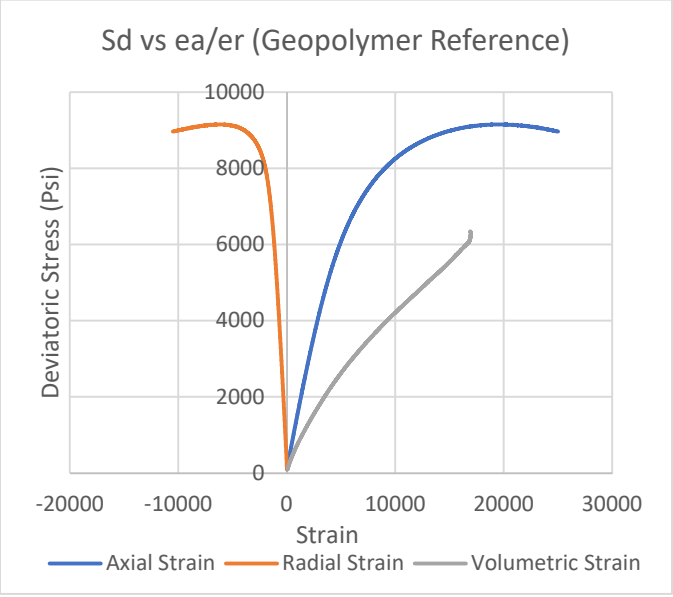

Figure 10 Stress vs Strain curve - Geopolymer Reference

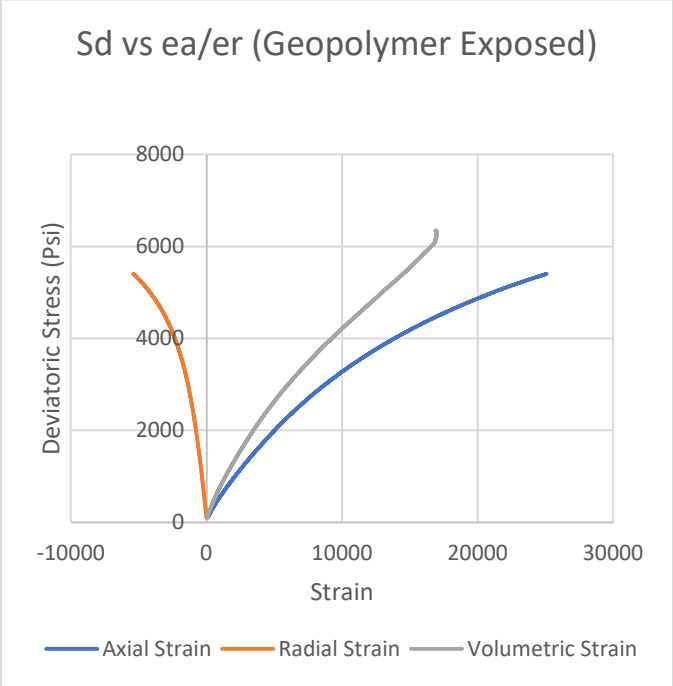

Figure 11 Stress vs Strain curve - Geopolymer Exposed

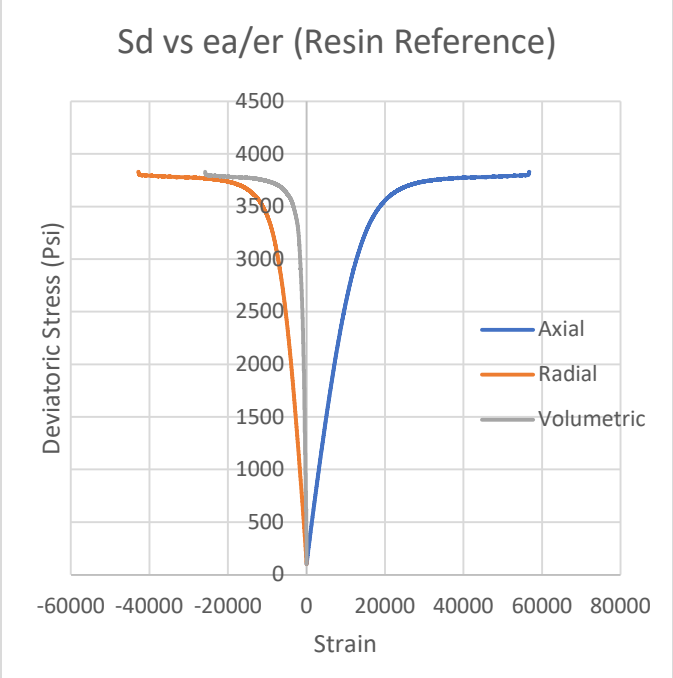

Figure 12 Stress vs Strain curve - Resin Reference

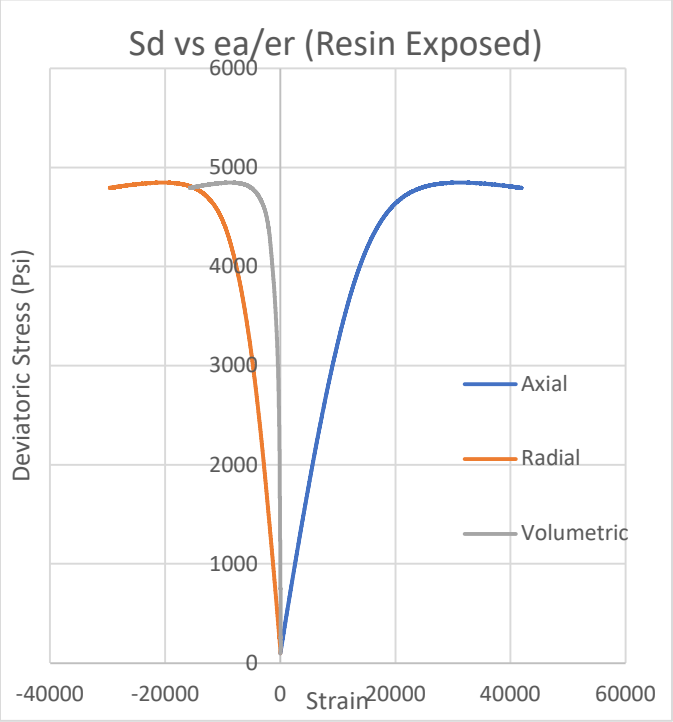

Figure 13 Stress vs Strain curve - Resin Exposed

The volumetric strain governs how materials distribute applied loads, where a high volumetric strain signifies material deformation under stress, reducing its load-bearing ability. Materials that do not maintain volume under loading risk structural failure, with excessive volumetric strain leading to cracks. Stress versus volumetric strain graphs for cement emphasize the roles of axial strain (deformation along the sample's length under uniaxial compression) and radial strain (perpendicular deformation). When axial strain exceeds radial strain, it reflects greater longitudinal compression and causes volumetric strain to shift positively, indicating compaction or volume decrease. This volume reduction occurs as the cement matrix compresses longitudinally more than it expands laterally, reducing void spaces and densifying the material. This behavior corresponds to diminished volumetric dilation, meaning the cement undergoes plastic deformation, absorbing stress without volumetric expansion. During this plastic phase, the material sustains significant strain without cracking through internal structural rearrangements that favor shear flow instead of crack propagation.

Conclusions

This study highlights the practical significance and suitability of various oilwell cements for long-term wellbore integrity in CCS projects by demonstrating their resilience to supercritical CO_2 exposure.

The findings show that both formulations show a roughly 3% drop in porosity, with a continuous trend of decreasing porosity in Class C and Class H samples. On the other hand, the geopolymer cement's porosity dramatically increases from 10.8% to 40.8. This rise is explained by the special pozzolanic reactions in fly ash when exposed to CO_2, resulting in extensive mineral phases and interconnected pore networks. By filling gaps, the carbonation reaction—in which CO_2 combines with calcium hydroxide to generate calcium carbonate—usually decreases porosity in conventional cement. Still, it can also increase porosity in geopolymer cement by dissolving certain phases.

Resin-based cements are generally more compliant than Class H well cement, which leads to distinct mechanical contrasts: resin cements typically exhibit lower compressive strength and a smaller Young's modulus, meaning they deform more under the same applied stress, while also showing a higher Poisson's ratio, so they tend to exhibit greater lateral strain for a given axial compression. Class H well cement, engineered for downhole applications, is formulated for higher compressive strength and stiffness (higher Young's modulus) and usually has a lower Poisson's ratio (commonly around 0.20–0.30), giving it superior resistance to axial deformation and reduced lateral expansion under load. These inherent material differences influence performance in wellbore environments; the stiffer Class H cement better supports casing and resists borehole collapse and excessive deformation, whereas resin cements, with their greater elasticity, may absorb strains without brittle failure but provide less structural support under high compressive loads. In applications where load-bearing capacity and rigidity are critical, Class H is preferred, while resin-based systems can be advantageous where flexibility, crack tolerance, and energy absorption are priorities. Ultimately, selecting between resin and Class H cement requires balancing stiffness, strength, and deformation behavior against operational needs such as zonal isolation, stress conditions, and long-term durability; designers should evaluate modulus, Poisson's ratio, and peak strength alongside environmental factors to optimize cement choice for specific well conditions.

Acknowledgments

The authors acknowledge the support from Mr. Casey Bristow and Mr. Brad Pruett from Riteks in providing the Resin cement samples. The authors would like to thank Mr. Cecil Millikan and the Bob L Herd Department of Petroleum Engineering at the Texas Tech University for their assistance in the experiments.

References

API, A. P. I. (1998). *API RP 40 - Recommended Practices for Core Analysis*.

Ati, C. D. (2004). Carbonation-Porosity-Strength Model for Fly Ash Concrete. *Journal of Materials in Civil Engineering*, *16*(1), 91–94. https://doi.org/10.1061/(asce)0899-1561(2004)16:1(91)

Carroll, S., Carey, J. W., Dzombak, D., Huerta, N. J., Li, L., Richard, T., Um, W., Walsh, S. D. C. & Zhang, L. (2016). Review: Role of chemistry, mechanics, and transport on well integrity in CO2 storage environments. *International Journal of Greenhouse Gas Control*, *49*, 149–160. https://doi.org/10.1016/j.ijggc.2016.01.010

Corvisier, J., Brunet, F., Fabbri, A., Bernard, S., Findling, N., Rimmelé, G., Barlet-Gouédard, V., Beyssac, O. & Goffé, B.

(2010). Raman mapping and numerical simulation of calcium carbonates distribution in experimentally carbonated Portland-cement cores. *European Journal of Mineralogy*, *22*(1), 63–74. https://doi.org/10.1127/0935-1221/2010/0022-1977

Fentaw, J. W., Emadi, H., Hussain, A., Fernandez, D. M. & Thiyagarajan, S. R. (2024). Geochemistry in Geological CO2 Sequestration: A Comprehensive Review. *Energies*, *17*(19), 5000. https://doi.org/10.3390/en17195000

García-González, C. A., Hidalgo, A., Fraile, J., López-Periago, A. M., Andrade, C. & Domingo, C. (2007). Porosity and Water Permeability Study of Supercritically Carbonated Cement Pastes Involving Mineral Additions. *Industrial & Engineering Chemistry Research*, *46*(8), 2488–2496. https://doi.org/10.1021/ie061571o

Gasda, S. E., Bachu, S. & Celia, M. A. (2004). Spatial characterization of the location of potentially leaky wells penetrating a deep saline aquifer in a mature sedimentary basin. *Environmental Geology*, *46*(6–7), 707–720. https://doi.org/10.1007/s00254-004-1073-5

Khalifeh, M., Saasen, A., Vralstad, T. & Hodne, H. (2014). Potential utilization of class C fly ash-based geopolymer in oil well cementing operations. *Cement and Concrete Composites*, *53*, 10–17. https://doi.org/10.1016/j.cemconcomp.2014.06.014

Kutchko, B. G., Strazisar, B. R., Lowry, G. V., Dzombak, D. A. & Thaulow, N. (2008). Rate of CO2 Attack on Hydrated Class H Well Cement under Geologic Sequestration Conditions. *Environmental Science & Technology*, *42*(16), 6237–6242. https://doi.org/10.1021/es800049r

Palomo, A., Grutzeck, M. W. & Blanco, M. T. (1999). Alkali-activated fly ashes A cement for the future. *Cement and Concrete Research*, *29*(8), 1323–1329. https://doi.org/10.1016/s0008-8846(98)00243-9

Panduro, E. A. C., Cordonnier, B., Gawel, K., Børve, I., Iyer, J., Carroll, S. A., Michels, L., Rogowska, M., McBeck, J. A., Sørensen, H. O., Walsh, S. D. C., Renard, F., Gibaud, A., Torsæter, M. & Breiby, D. W. (2020). Real Time 3D Observations of Portland Cement Carbonation at CO2 Storage Conditions. *Environmental Science & Technology*, *54*(13), 8323–8332. https://doi.org/10.1021/acs.est.0c00578

Ridha, S., Setiawan, R. A., Hamid, A. I. A. & Shahari, A. R. (2018). The influence of CO2 accelerated carbonation on alkali-activated fly ash cement under elevated temperature and pressure. *Materialwissenschaft Und Werkstofftechnik*, *49*(4), 483–488. https://doi.org/10.1002/mawe.201800029

Ridha, Syahrir, Setiawan, R. A., Pramana, A. A. & Abdurrahman, M. (2020). Impact of wet supercritical CO2 injection on fly ash geopolymer cement under elevated temperatures for well cement applications. *Journal of Petroleum Exploration and Production Technology*, *10*(2), 243–247. https://doi.org/10.1007/s13202-019-0693-y

Ryu, G. S., Lee, Y. B., Koh, K. T. & Chung, Y. S. (2013). The mechanical properties of fly ash-based geopolymer concrete with alkaline activators. *Construction and Building Materials*, *47*, 409–418. https://doi.org/10.1016/j.conbuildmat.2013.05.069

Sauki, A. & Irawan, S. (2010). Effects of Pressure and Temperature on Well Cement Degradation by Supercritical CO2 - UTP Scholarly Publication. *Int. J. Eng. Technol.*, 53–61. http://eprints.utp.edu.my/id/eprint/4729/

Strazisar, B., Kutchko, B. & Huerta, N. (2009). Chemical Reactions of Wellbore Cement Under CO2 Storage Conditions: Effects of Cement Additives. *Energy Procedia*, *1*(1), 3603–3607. https://doi.org/10.1016/j.egypro.2009.02.155